

AD-A193 386

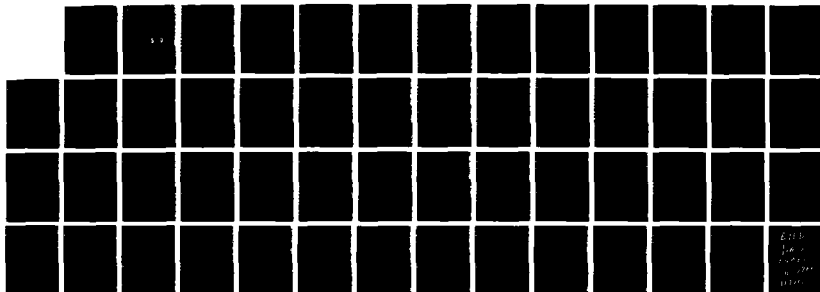
THEORY OF SOUND PRODUCTION BY VORTEX-AIRFOIL
INTERACTION(U) BBN LABS INC CAMBRIDGE MA M S HOWE
JAN 88 BBN-6710 N00167-87-C-0021

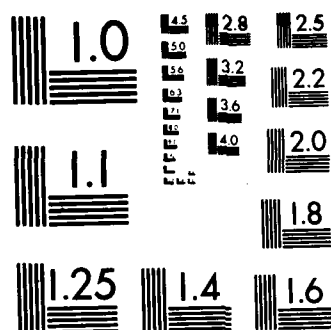
1/1


UNCLASSIFIED

F/G 20/1

NL






 MICROCOPY RESOLUTION TEST CHART
 NATIONAL BUREAU OF STANDARDS-1963-A

BBN Laboratories Incorporated

A Subsidiary of Bolt Beranek and Newman Inc.

Report No. 6710

DTIC FILE COPY

AD-A193 386

THEORY OF SOUND PRODUCTION BY VORTEX-AIRFOIL INTERACTION

M.S. Howe

Contract No. N00167-87-C-0021

January 1988

DTIC
ELECTE
MAR 30 1988
S A D

Prepared by:

BBN Laboratories Incorporated
10 Moulton Street
Cambridge, MA 02238

DISTRIBUTION STATEMENT A

Approved for public release
Distribution Unlimited

Prepared for:

Office of Naval Research
Applied Hydrodynamics Research Program
Arlington, VA 22217
Attn: James A. Fein

88 1 27 186

Report No. 6710

THEORY OF SOUND PRODUCTION BY VORTEX-AIRFOIL INTERACTION

M.S. Howe

Contract No. N00167-87-C-0021

January 1988

Prepared by:

BBN Laboratories Incorporated
10 Moulton Street
Cambridge, MA 02238

Prepared for:

Office of Naval Research
Applied Hydrodynamics Research Program
Arlington, VA 22217
Attn: James A. Fein

Accession For	
NTIS CRA&I	<input checked="checked" type="checkbox"/>
DTIC TAB	<input type="checkbox"/>
Unannounced	<input type="checkbox"/>
Justification	
By <i>pr. etc.</i>	
Distribution/	
Availability Codes	
Dist	Availability for Special
A-1	



SUMMARY

An analysis is made of the sound produced when a field of vorticity is cut by an airfoil in low Mach number flow. A general formula is given for the acoustic pressure when the airfoil is rigid and the chord is acoustically compact. This expresses the radiation in terms of an integral over the region occupied by the vorticity; the integrand contains factors describing the influence of the thickness, twist and camber of the airfoil. Explicit analytical results are derived for the case of a rectilinear vortex, having small core diameter and finite axial velocity defect, which is "chopped" by an airfoil of large aspect ratio. The acoustic signature generally comprises two components associated respectively with the axial and azimuthal vorticity, the latter being determined by the velocity defect distribution within the core. Sound is generated predominantly when the core is in the neighborhoods of the leading and trailing edges. The contribution from the trailing edge is usually small, however, because of destructive interference between sound produced by edge-diffraction of near field energy of the vortex and that produced by vorticity shed into the wake of the airfoil in order to satisfy the unsteady Kutta condition that the pressure and velocity should be bounded at the edge. When the shed vorticity is assumed to convect at the same mean stream velocity as the impinging vortex, the interference is predicted to be complete, and no trailing edge sound is generated. If the shed vorticity is taken to convect at a reduced, "near wake" velocity, which might be appropriate for small scale structures comparable in size to the diameter of the vortex core, a small but non-negligible pressure pulse is radiated from the trailing edge. A tentative comparison with experiment appears to confirm the presence of this trailing edge pulse.

TABLE OF CONTENTS

	page
SUMMARY.....	ii
SECTION 1. INTRODUCTION.....	1
2. GENERAL REPRESENTATION OF SOUND PRODUCED BY VORTICITY IN THE VICINITY OF AN AIRFOIL OF COMPACT CHORD.....	5
2.1 Aerodynamic Sound in Low Mach Number Flow.....	5
2.2 The Low Frequency Green's Function.....	8
2.3 Modeling the Convection of Vorticity...	9
3. SOUND PRODUCED BY UNIFORMLY CONVECTING VORTICITY IMPINGING ON A THIN AIRFOIL OF INFINITE SPAN.....	12
3.1 The Directly Generated Sound.....	12
3.2 The Radiation Produced by the Shed Vorticity.....	15
3.3 Summary of Results.....	21
4. ANALYTICAL SPECIFICATION OF A RECTILINEAR VORTEX.....	22
5. VORTEX CHOPPING NOISE.....	26
5.1 Sound Generated by the Axial Component of Vorticity $\underline{\Omega}_T$	26
5.2 Sound Generated by the Axial Velocity Defect in the Core ($\underline{\Omega}_A$)	31
6. APPLICATION TO ROTOR-VORTEX INTERACTION NOISE.....	37
7. CONCLUSION.....	45
REFERENCES.....	48

1. INTRODUCTION

An airfoil which is in an accelerated, subsonic motion through a nominally quiescent fluid produces sound because of the unsteady forces exerted on the fluid. These forces behave as acoustic sources of dipole type, with dipole axis coinciding with the line of action of a force. Thus, the radiation from a propeller is associated principally with a system of dipoles whose axes are normal to the plane of rotation; the dipoles correspond to the distributed lift (or "thrust") forces experienced by the propeller blades, each of which is accelerating in a circle (Gutin 1948). The lift (and drag) forces also vary when the airfoil encounters a region of unsteady fluid motion, either turbulent or organized. In an unbounded medium, the unsteadiness is indicative of the presence of vorticity in the vicinity of the airfoil, and the impinging, unsteady motion is usually called a gust. The lift exerted on an airfoil by a time-harmonic gust in incompressible flow was first examined theoretically by von Karman and Sears (1938).

There are many practical problems in which the gust can be attributed to a relatively simple distribution of vorticity. For example, a tip vortex shed from a blade of the main rotor of a helicopter can impinge on the following blade, producing a characteristic noise often referred to as "blade slap" (Schmitz and Yu 1986). This phenomenon, in which the vortex and the following blade are approximately in parallel planes of mean motion, has been examined theoretically by Martinez and Widnell (1983), Lee and Roberts (1985), and by Hardin and Lamkin (1987). Similarly, when the helicopter is in forward flight, the main rotor tip vortices can be sucked through the tail rotor disc. In that case, the axes of the ingested vortices are almost normal to the disc plane, and sound is produced by the multiple "chopping" of the vortex cores by the blades of the tail rotor. According

to Leverton, Pollard and Wills (1977), the sound produced in this manner can often dominate the main rotor and engine noise during helicopter landing maneuvers.

Schlinker and Amiet (1983) and Ahmadi (1986) have recently undertaken similar, but independent experimental studies of the sound produced by the chopping of a vortex. In both investigations, a nominally rectilinear vortex was generated in an open-jet wind tunnel, with the axis of the vortex parallel to the flow, by vorticity shed from the tip region of a stationary airfoil. The vortex impinged on a rotor located downstream whose disc plane is orientated normal to the mean flow. Measurements were made of the impulsive sound produced when the vortex core is chopped by the rotor blades, and of the various geometrical and aerodynamic parameters which are needed to quantify the details of the interaction of the vortex and the blades.

Amiet (1986) has proposed a theory to account for the sound generated in these experiments that is based on previous studies of the gust interaction problem for an airfoil modelled by a flat plate of infinite span (see, e.g., Amiet 1974, 1976). It was assumed that the mean axial velocity in the core of the vortex was equal to that in the ambient, mean wind tunnel flow. However, the observations of Schlinker and Amiet (1983) and of Ahmadi (1986) indicate the existence of a velocity defect within the core, the peak axial velocity often being as much as 10% smaller than the mean wind tunnel velocity. Schlinker and Amiet (1983) argued that a defect of this magnitude was too small to affect the level and characteristic signature of the acoustic radiation. On the other hand, in the absence of a velocity defect the theoretical calculations (Amiet 1986) revealed that no sound is produced when the mean chord of the airfoil is at right angles to the vortex axis, although in these circumstances a finite axial flow defect would still be expected to generate sound.

In this paper a general theory is proposed for the sound produced when a field of vorticity in low subsonic mean flow is cut by an arbitrary, rigid airfoil of acoustically compact chord (i.e., when the wavelength of the generated sound greatly exceeds the chord). The radiation is expressed directly in terms of the vorticity and, although applicable to flows with quite general distributions of vorticity, the theory is especially suited to problems involving discrete or localized vortex elements. In particular, the influence of an axial velocity defect within the core of a rectilinear vortex, which determines an azimuthal component of vorticity within the core, can be treated theoretically in a manner entirely analogous to the treatment of the conventional axial vorticity component. The details of this case will be worked out for vortex-airfoil interactions in free space, but the method to be described is readily extended to problems involving, say, the interaction of helical tip vortices in duct flows with downstream control surfaces.

There are distinct advantages of confining the discussion to airfoils of compact chord. In the first instance, there is a large body of applications in hydroacoustics for which a general treatment of the compressible flow in the vicinity of the airfoil would be unnecessarily complicated. Secondly, it enables the radiation to be expressed analytically in closed form and the various different contributing sources to be identified. In addition, the role of the unsteady Kutta condition (that the velocity and pressure should remain finite at the trailing edge of the airfoil), and the significance of the near wake convection velocity can be examined in detail. It will be shown, for example, that, for a flat airfoil of uniform chord and large span, the sound produced by vorticity shed from the trailing edge in order to satisfy the Kutta condition, interferes destructively with the "direct" sound generated by the impinging vorticity when near field energy of the latter is diffracted at the trailing

edge. When the shed vorticity is assumed to convect at the same mean stream velocity as the impinging vorticity, the destructive interference is total, and no sound emanates from the trailing edge region. When the shed vorticity convects at a smaller, near-wake velocity, however, the trailing edge radiation is small, but finite.

The aerodynamic sound problem for a general airfoil of compact chord is formulated and solved in Section 2. In Section 3 the results are specialized to a thin airfoil of essentially constant chord and large aspect ratio at zero angle of attack, and the impinging vorticity is assumed to convect in a frozen pattern at the velocity of the mean stream. Analytical representations of the acoustic radiation produced by a rectilinear vortex with axial velocity defect are derived in Sections 4 and 5. In Section 6 a tentative comparison is made of predictions with the vortex-rotor interaction noise measurements of Schlinker and Amiet (1983).

2. GENERAL REPRESENTATION OF SOUND PRODUCED BY VORTICITY IN THE VICINITY OF AN AIRFOIL OF COMPACT CHORD

2.1 Aerodynamic Sound in Low Mach Number Flow

Consider the generation of sound by an inhomogeneous field of vorticity convected in low Mach number, high Reynolds number flow past a stationary, rigid airfoil. The characteristic wavelength of the sound is assumed to be large relative to the chord of the airfoil. Let the fluid have mean density ρ_0 and sound speed c , and let the mean flow be at speed U in the positive x_1 -direction of a rectangular coordinate system (x_1, x_2, x_3) . The origin of coordinates is located at some convenient point within the airfoil; the x_3 -axis is taken in the spanwise direction, and the x_2 -axis is vertically "upwards," at right angles to the mean flow, as illustrated in Figure 1.

When the Mach number $M = U/c$ is sufficiently small relative to unity that the convection and scattering of sound by the mean flow can be ignored, the generation of sound by the unsteady flow is governed by the solution of the inhomogeneous wave equation

$$\{\partial^2/c^2 \partial t^2 - \nabla^2\}B = \text{div}(\underline{\omega} \underline{\hat{v}}) , \quad (2.1)$$

(Howe 1975), where t denotes time, $\underline{v} = \underline{v}(\underline{x}, t)$ the velocity, $\underline{\omega} = \text{curl } \underline{v}$ the vorticity, and B is the stagnation enthalpy defined in uniform, homentropic flow by

$$B = \int dp/\rho + v^2/2 , \quad (2.2)$$

p being the pressure and $\rho = \rho(p)$ the local density. At large distances from the airfoil, in the acoustic far field, the perturbation values of the pressure $p(\underline{x}, t)$ and the stagnation enthalpy $B'(\underline{x}, t)$, say, are related by

$$B'(\underline{x}, t) = p(\underline{x}, t) / \rho_0, \quad M \ll 1. \quad (2.3)$$

Equation (2.1) is to be solved for B in terms of the aeroacoustic source $\underline{\omega}^* \underline{v}$, whose properties are specified, or have been determined by prior analysis. The solution must satisfy the radiation condition of outgoing waves at large distances from the airfoil, and comply with the rigid boundary condition that the normal velocity on the airfoil v_n , say, vanishes.

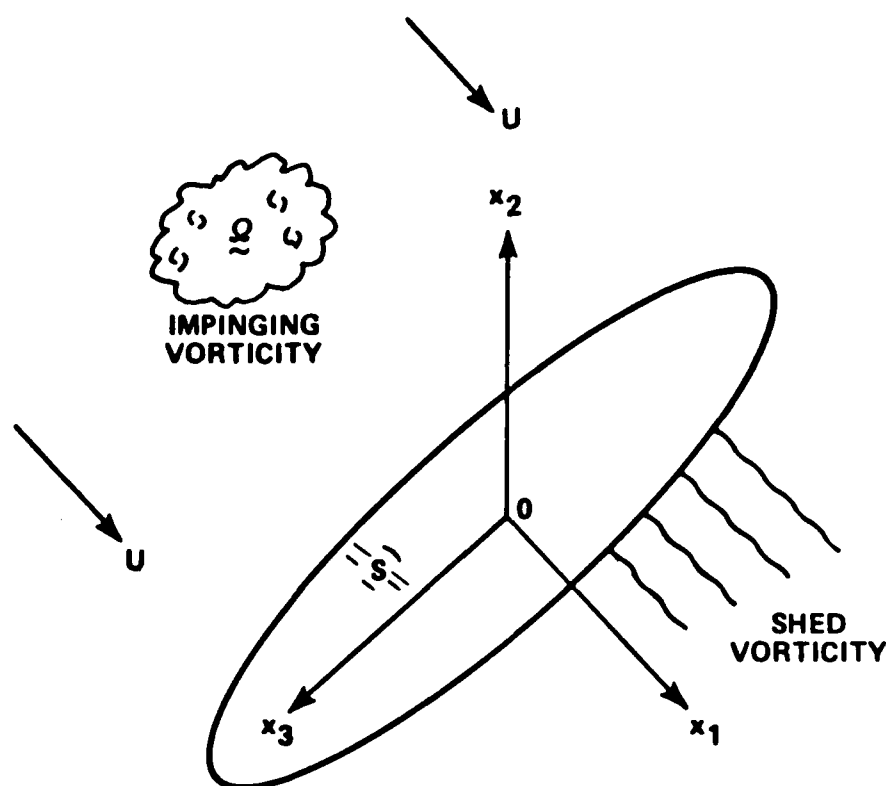


FIGURE 1. CONVECTION AND SHEDDING OF VORTICITY IN MEAN FLOW PAST THE AIRFOIL.

A formal representation of the solution can be written down by introducing a Green's function $G(\underline{x}, \underline{y}; t, \tau)$, which is the solution of (2.1) with outgoing wave behavior when the right hand side is replaced by the impulsive point source $\delta(\underline{x} - \underline{y})\delta(t - \tau)$. If G is defined to have vanishing normal derivative $\partial G / \partial x_n$ on the airfoil (and therefore, by reciprocity, such that $\partial G / \partial y_n = 0$, where x_n, y_n are directed into the fluid) it follows by routine application of Green's theorem (Stratton 1941) that

$$B(\underline{x}, t) = - \oint_S G(\underline{x}, \underline{y}; t, \tau) \left\{ \frac{\partial B}{\partial y_n}(\underline{y}, \tau) + (\underline{\omega} \wedge \underline{v})_n(\underline{y}, \tau) \right\} dS(\underline{y}) d\tau \\ - \int (\underline{\omega} \wedge \underline{v})(\underline{y}, \tau) \cdot \frac{\partial G}{\partial \underline{y}}(\underline{x}, \underline{y}; t, \tau) d^3 \underline{y} d\tau. \quad (2.4)$$

In this expression the first integral on the right hand side is taken over the surface S of the airfoil (with surface element $dS(\underline{y})$), the normal component $(\underline{\omega} \wedge \underline{v})_n$ being directed into the fluid. The second integral is over the region of space within which $\underline{\omega} \neq 0$.

To simplify (2.4) we note that in high Reynolds number, homentropic flow the momentum equation can be expressed in the form

$$\partial \underline{v} / \partial t + \nabla B + \underline{\omega} \wedge \underline{v} = 0 \quad (2.5)$$

Since $v_n = 0$ on the airfoil, it follows that the surface integral in (2.4) may be discarded, yielding

$$B(\underline{x}, t) = - \int (\underline{\omega} \wedge \underline{v})(\underline{y}, \tau) \cdot \frac{\partial G}{\partial \underline{y}}(\underline{x}, \underline{y}; t, \tau) d^3 \underline{y} d\tau. \quad (2.6)$$

The volume integral is taken over fluid elements where $\underline{\omega} \neq 0$. This comprises the region containing the incident vorticity and that occupied by vorticity shed from the airfoil. The latter

includes vorticity shed from the trailing edge in response to excitation by the impinging vorticity, together with tip vortices when the airfoil is at a finite angle of attack. In regions where $\underline{\omega} = \underline{0}$ equations (2.5), (2.6) imply that the unsteady velocity component is equal to $\nabla\phi$, where the potential ϕ satisfies $\partial\phi/\partial t = -B$.

2.2 The Low Frequency Green's Function

In aerodynamic sound problems involving the interaction of low Mach number vortical flow with a solid body, the wavelength of the principal ("dipole") component of the generated sound greatly exceeds the length scale of variation of the geometric features of the body. These variations may be regarded as surface inhomogeneities at which a small fraction of the near field ("hydrodynamic") energy of the vortex system is diffracted into sound. In these circumstances the Green's function $G(\underline{x}, \underline{y}; t, \tau)$ can be taken in its low frequency form (as discussed in detail by Howe 1975). In the case of an airfoil of compact chord, and when the observation point \underline{x} is in the acoustic far field, this is given by

$$G(\underline{x}, \underline{y}; t, \tau) = \frac{1}{4\pi|\underline{x}-\underline{y}|} \delta\{t-\tau-|\underline{x}-\underline{y}|/c\} , \quad |\underline{x}| \rightarrow \infty, M \ll 1 , \quad (2.7)$$

where $Y_i = Y_i(\underline{y})$ is equal to the velocity potential of an hypothetical incompressible flow in the i -direction which has unit speed at large distances from the airfoil (i.e., such that $Y_i \rightarrow y_i$ at large distances). Observe that, since $\partial G/\partial y_n \sim \partial Y/\partial y_n$, the normal derivative condition $\partial G/\partial y_n = 0$ on the airfoil is satisfied provided the potential functions Y_i satisfy this condition.

Making use of (2.7) in the integrand of (2.6) we find (from (2.3)) that the acoustic pressure fluctuations at large distances from the airfoil are given by

$$p(\underline{x}, t) = \frac{-\rho_0 \underline{x}_i}{4\pi c |\underline{x}|^2} \frac{\partial}{\partial t} \int (\underline{\omega} \cdot \underline{v})_j(\underline{y}, t - |\underline{x} - \underline{y}|/c) \frac{\partial Y_i}{\partial y_j}(\underline{y}) d^3 \underline{y} . \quad (2.8)$$

The proportionality of this result to the direction cosine $\underline{x}_i/|\underline{x}|$ indicates that the component of the radiation which involves Y_i is generated by dipole sources orientated in the i -direction. The components Y_1, Y_3 account for sound produced as a result of the finite thickness, camber, twist and angle of attack of the airfoil. Note that, since the airfoil has compact chord, we can take $\underline{y} = (0, 0, y_3)$ in the retarded time argument $[t] = t - |\underline{x} - \underline{y}|/c$ of (2.8). This is an adequate approximation provided that the distance from the airfoil of vorticity at the retarded position $(\underline{y}, [t])$ of space-time is much smaller than a characteristic wavelength of the sound it is producing. But this is always the case when the radiation is generated, as here, by the motion at low Mach numbers of the near field of the vorticity in the vicinity of the airfoil.

2.3 Modeling the Convection of Vorticity

Equation (2.8) expresses the acoustic pressure in terms of the retarded distributions of vorticity and local convection velocity \underline{v} . In low Mach number flows the functional forms of these quantities may be determined to a sufficient approximation by analytical or numerical integration of the equations of incompressible flow. Hardin and Lamkin (1987), for example, have used a numerical integration scheme to treat an analogous problem of sound production by convected discrete vortex elements. For a thin airfoil at small angle of attack, a first approximation

would be to assume that vorticity is swept past the airfoil in a frozen pattern at the velocity of the undisturbed mean flow. According to Goldstein and Atassi (1976) this procedure yields reasonable predictions when the hydrodynamic wavelength of the vorticity greatly exceeds the thickness of the airfoil.

When a rectilinear vortex is chopped by an airfoil moving parallel to a plane whose normal is nearly aligned with the axis of the vortex, the length scale of the vorticity in the chordwise direction is equal to the vortex core diameter. This is typically much smaller than the chord, and finite values of the camber, twist, thickness, and angle of attack would then be expected to result in the distortion of the vortex, and perhaps also in the generation of bending waves which propagate along the vortex axis (Leibovich, Brown and Patel 1986). This could have a significant effect on the acoustic signature, especially in radiation directions parallel to the mean plane of the airfoil. Accordingly, an accurate characterization of the radiated sound is possible only after a detailed investigation of the dynamics of the vortex-airfoil interaction has been performed.

In the following these difficulties will be avoided by adopting the approach of thin airfoil theory (Ashley and Landahl 1985), and specifically by modeling the airfoil as a flat, rigid lamina at zero angle of attack. The tip vortices which generate the mean lift are then absent and, provided the mean velocity is large compared to the perturbation velocities induced by the impinging vortex, and in particular relative to the upwash component of velocity (normal to the plane of the airfoil), it is permissible to assume that the vortex will be convected parallel to the x_1 -axis at the undisturbed mean flow speed U . Thin airfoil theory determines the strength of the additional vorticity which is shed from the trailing edge during the interaction by application of the unsteady Kutta condition, and

assumes that it is also convected at speed U . The length scale of the shed vorticity must be of the same order as the diameter of the vortex core. However, if this is much smaller than the chord of the airfoil, it is arguably more appropriate to require the convection velocity in the wake just downstream of the trailing edge to be equal to a near wake mean velocity $U_c < U$.

3. SOUND PRODUCED BY UNIFORMLY CONVECTING VORTICITY IMPINGING ON A THIN AIRFOIL OF INFINITE SPAN

3.1 The Directly Generated Sound

The frozen field of vorticity

$$\underline{\omega} = \underline{\Omega}(x_1 - Ut, x_2, x_3) , \quad (3.1)$$

is assumed to convect at the uniform mean stream velocity U and to be cut by an airfoil which is idealized as a thin, rigid lamina at zero angle of attack. We then have

$$Y_1 = y_1, \quad Y_2 = Y_2(\underline{y}), \quad Y_3 = y_3 , \quad (3.2)$$

where $Y_2(\underline{y})$ is the velocity potential of incompressible flow in the 2-direction which has unit speed at large distances from the airfoil. The identity $\underline{\omega} \cdot \underline{v} = (\underline{v} \cdot \nabla) \underline{v} - \nabla(v^2/2)$, and the rigid surface condition $v_n = 0$, then imply that only the y_2 -dipole makes a finite contribution to the radiation integral (2.8), which now assumes the form

$$\underline{p}(x, t) = \frac{-\rho_o U \cos \bar{\theta}}{4\pi c |\underline{x}|} \frac{\partial}{\partial t} \int \left\{ \Omega_3(\underline{y}, [t]) \frac{\partial Y_2}{\partial y_2} - \Omega_2(\underline{y}, [t]) \frac{\partial Y_2}{\partial y_3} \right\} d^3 \underline{y} , \quad (3.3)$$

where $\bar{\theta} = \cos^{-1}(x_2/|\underline{x}|)$ is the angle between the radiation direction \underline{x} and the normal to the airfoil (the x_2 -axis).

For an airfoil of large aspect ratio $\partial Y_2 / \partial y_3 \ll \partial Y_2 / \partial y_2$ except in the immediate neighborhoods of the airfoil tips. The second term in the brace brackets of the integrand of (3.3) may then be discarded. If the vortex-airfoil interaction occurs at a sufficient distance from the tips that the chord may be assumed

to be uniform and to occupy the interval $|x_1| < a$ of the x_2 -plane (see Figure 2), we may then take

$$\left. \begin{array}{l} y_2 = \operatorname{Re}\{-i(z_0^2 - a^2)^{1/2}\} , \\ \text{where} \\ z_0 = y_1 + iy_2 . \end{array} \right\} \quad (3.4)$$

The use of this approximation is tantamount to assuming the airfoil to have infinite span.

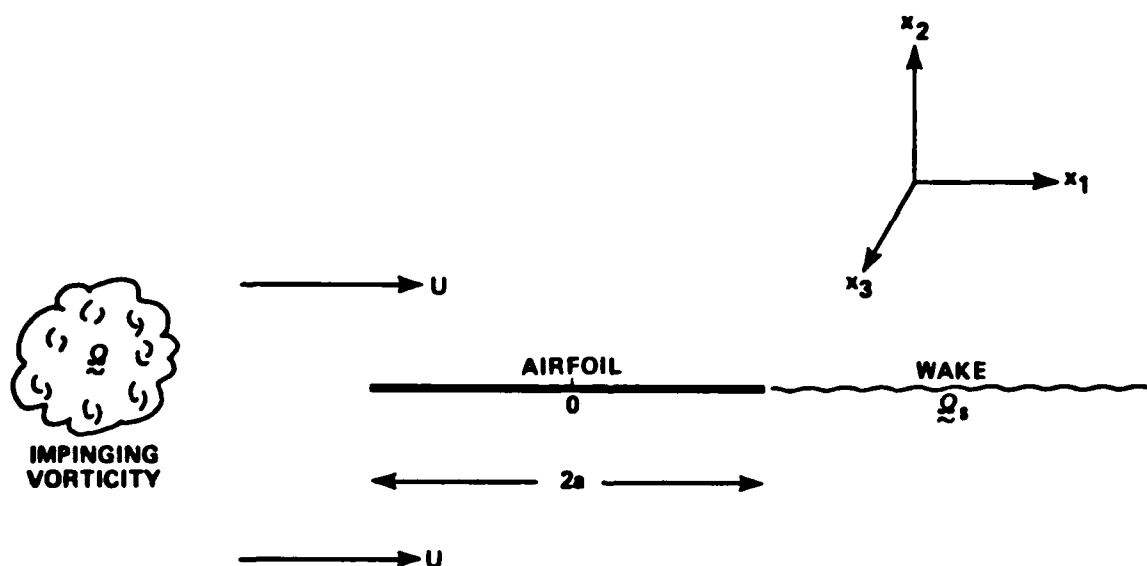


FIGURE 2. CONFIGURATION OF THE INTERACTION PROBLEM FOR AN AIRFOIL OF INFINITE ASPECT RATIO.

Let us next suppose that the vorticity $\underline{\Omega}$ impinges on the airfoil in an acoustically compact neighborhood of $x_3 = 0$, so that the retarded time may be taken to be $[t] = t - |\underline{x}|/c$. Define the Fourier transform $\hat{\Omega}_3(\underline{K})$, $\underline{K} = (K_1, K_2, K_3)$ of Ω_3 relative to a coordinate system \underline{x}' , say, that is translating uniformly at speed U in the x_1 -direction, i.e., such that

$$\left. \begin{aligned} \hat{\Omega}_3(\underline{K}) &= \frac{1}{(2\pi)^3} \int_{-\infty}^{\infty} \Omega_3(\underline{x}') e^{-i\underline{K} \cdot \underline{x}'} d^3 \underline{x}' , \\ \underline{x}' &= \underline{x} - (Ut, 0, 0) . \end{aligned} \right\} \quad (3.5)$$

Then

$$\Omega_3(x_1 - Ut, x_2, x_3) = \frac{1}{U} \int_{-\infty}^{\infty} \hat{\Omega}_3(\omega/U, K_2, K_3) e^{i\{\underline{K} \cdot \underline{x} - \omega t\}} d\omega dK_2 dK_3 , \quad (3.6)$$

where we have introduced the radian frequency $\omega = UK_1$ of the constituent components of the radiation field.

Inserting this representation into (3.3) (with the second term in the brace brackets discarded), we obtain

$$\begin{aligned} p_{\Omega}(\underline{x}, t) &= \frac{-\rho_0 \cos \bar{\theta}}{2c|\underline{x}|} \frac{\partial}{\partial t} \int \hat{\Omega}_3(\omega/U, K_2, 0) \frac{\partial Y_2}{\partial y_2}(y_1, y_2) \\ &\quad \times \exp\{i(\omega y_1/U + K_2 y_2 - \omega[t])\} d\omega dK_2 dy_1 dy_2 , \end{aligned} \quad (3.7)$$

wherein the notation $p_{\Omega}(\underline{x}, t)$ signifies the acoustic pressure fluctuations generated directly by the impinging vorticity $\underline{\Omega}$, with no account taken of the coherent radiation from the vorticity $\underline{\Omega}_s$, say, shed into the wake. When y_2 is defined as in (3.4), the remaining integrations with respect to y_1, y_2 are readily evaluated (divergent integrals being treated as

generalized functions, Lighthill 1958) by making use of an integral definition of the Bessel function $J_1(x)$ given in Abramowitz and Stegun (1972, Section 9). This yields

$$p_{\Omega}(\underline{x}, t) = \frac{\pi \rho_0 a U \cos \bar{\theta}}{c |\underline{x}|} \frac{\partial}{\partial t} \int_{-\infty}^{\infty} \frac{\omega \hat{\Omega}_3(\omega/U, K_2, 0) J_1(\omega a/U) e^{-i\omega[t]}}{(\omega^2 + U^2 K_2^2)} dK_2 d\omega. \quad (3.8)$$

3.2 The Radiation Produced by the Shed Vorticity

The strength of the vorticity shed into the wake is determined by application of the unsteady Kutta condition, that the perturbation velocity and pressure are finite at the trailing edge. This will be satisfied provided that B and $\partial B / \partial x_2$ are finite. Consider first the contribution to B from the Fourier component

$$\frac{1}{U} \hat{\Omega}_3(\underline{K}) e^{i\{\underline{K} \cdot \underline{x} - \omega t\}}, \quad K_1 = \omega/U,$$

of (3.6), and note from (3.8) that, in calculating the resulting acoustic radiation, only components with $K_3 = 0$ need be considered.

Let $B'_{\Omega}(x_1, x_2) e^{-i\omega t}$ denote the corresponding component of the perturbation stagnation enthalpy. This can be calculated from equation (2.1) which assumes the locally two-dimensional form

$$\left. \begin{aligned} \{ \partial^2 / \partial x_1^2 + \partial^2 / \partial x_2^2 \} B'_{\Omega} &= - \frac{\partial q}{\partial x_2}, \\ q &= \hat{\Omega}_3(\omega/U, K_2, 0) e^{i\{\omega x_1/U + K_2 x_2\}} \end{aligned} \right\} \quad (3.9)$$

where, in addition, a further simplification has been introduced by noting that retarded times are negligible in the neighborhood of the airfoil. The solution of this equation is given by (2.6) with \underline{v} replaced by $(0, q, 0)$. The Green's function satisfies

$$\nabla^2 G = -\delta(\underline{x}-\underline{y})\delta(t-\tau) , \quad (3.10)$$

with $\partial G / \partial y_2 = 0$ on $|y_1| < a$, $y_2 = \pm 0$, and can be taken in the form (Milne-Thomson 1968, Section 8.71)

$$G = \frac{-1}{2\pi} \operatorname{Re} \{ \ln(\zeta - \zeta_0) + \ln(a^2 / \zeta^* - \zeta_0) \} \delta(x_3 - y_3) \delta(t - \tau) \quad (3.11)$$

where the asterisk denotes the complex conjugate, and

$$\left. \begin{aligned} \zeta &= z + (z^2 - a^2)^{1/2}, & z &= x_1 + ix_2, \\ \zeta_0 &= z_0 + (z_0^2 - a^2)^{1/2}, & z_0 &= y_1 + iy_2. \end{aligned} \right\} \quad (3.12)$$

It follows from these results that

$$B''_{\Omega} \approx C_{\Omega} + D_{\Omega} (x_1^2 - a^2)^{1/2} + \text{finite terms} , \quad (3.13)$$

$$x_1 \rightarrow a + 0, \quad x_2 = 0 ,$$

where C_{Ω} , D_{Ω} are independent of \underline{x} . In particular,

$$\frac{\partial B''_{\Omega}}{\partial x_2} \rightarrow \frac{a}{(x_1^2 - a^2)^{1/2}} \frac{\omega^2 \hat{\Omega}_3(\omega/U, K_2, 0) \{ J_0(\omega a/U) + iJ_1(\omega a/U) \}}{\{\omega^2 + U^2 K_2^2\}} \quad (3.14)$$

$$x_1 \rightarrow a + 0, \quad x_2 = 0 .$$

At a fixed value of the radian frequency ω , the aggregate contribution to $\partial B_{\Omega} / \partial x_2$ near the trailing edge is obtained by integrating over all values of K_2 :

$$\begin{aligned} \frac{\partial B'_{\Omega}}{\partial x_2} &= \int_{-\infty}^{\infty} \frac{\partial B'_{\Omega}}{\partial x_2} dK_2 \\ &= \frac{a}{(x_1^2 - a^2)^{1/2}} \int_{-\infty}^{\infty} \frac{\omega^2 \hat{\Omega}_3(\omega/U, K_2, 0) \{J_0(\omega a/U) + iJ_1(\omega a/U)\} dK_2}{\{\omega^2 + U^2 K_2^2\}}, \\ x_1 &+ a + 0, x_2 = 0. \end{aligned} \quad (3.15)$$

Turn attention now to the trailing edge motion induced by the shed vorticity $\underline{\Omega}_s$, which lies in the half-plane $x_1 > a$, $x_2 = 0$, and convects downstream at speed $U_c < U$. As before, only the Ω_{s3} component makes a finite contribution to the induced motion, and we may set

$$\Omega'_{s3}(\omega, K_3) = \gamma_0(\omega, K_3) H(x_1 - a) \delta(x_2) e^{i(\omega x_1/U_c + K_3 x_3 - \omega t)}, \quad (3.16)$$

where,

$$\Omega_{s3} = \int_{-\infty}^{\infty} \Omega'_{s3}(\omega, K_3) dK_3 d\omega, \quad (3.17)$$

$H(x)$ ($=1, 0$ according as $x \geq 0$) is the Heaviside unit function, and $\gamma_0(\omega, K_3)$ is to be determined.

For the purpose of computing the acoustic radiation attention may be confined to Fourier components with $K_3 = 0$. Let $B'_s e^{-i\omega t}$ denote the perturbation stagnation enthalpy near the trailing edge that is induced by the component $\Omega'_{s3}(\omega, 0)$. This is determined by the solution of

$$\{\partial^2/\partial x_1^2 + \partial^2/\partial x_2^2\}B'_S = -U_C \gamma_0 \frac{\partial}{\partial x_2} \{H(x_1-a)\delta(x_2)\exp(i\omega x_1/U_C)\} . \quad (3.18)$$

Now, except in the wake, $B'_S e^{-i\omega t} = -\partial \phi'_S / \partial t$, where ϕ'_S is the velocity potential of motion generated by the wake vorticity. The 3-component of the vortex strength of an element of the wake of length dx_1 is equal to $\gamma_0 dx_1 \exp\{i\omega(x_1/U_C - t)\}$. The evaluation of the contribution of each of these elements to the potential ϕ'_S , which must satisfy Kelvin's theorem that the circulation about the airfoil and wake is null, is a problem in classical hydrodynamics (Milne-Thomson 1968, Section 13.50), whose solution yields

$$\phi'_S = \frac{-\gamma_0}{2\pi} \int_a^\infty \operatorname{Re}\{i[\ln(\zeta-\xi) - \ln(\zeta-a^2/\xi)]\} e^{i\omega(y_1/U_C - t)} dy_1 , \quad (3.19)$$

where $\xi = y_1 + (y_1^2 - a^2)^{1/2}$, $\zeta = z + (z^2 - a^2)^{1/2}$, $z = x_1 + ix_2$.

When z lies in the vicinity of the trailing edge, the integral may be evaluated to give

$$B'_S \approx C_S + D_S (x_1^2 - a^2)^{1/2} + \dots, \quad x_1 \rightarrow a+0, \quad x_2 = 0 , \quad (3.20)$$

where C_S , D_S are constants, and specifically,

$$\frac{\partial B'_S}{\partial x_2} \approx \frac{a\omega\gamma_0}{4(x_1^2 - a^2)^{1/2}} \{H_0^{(1)}(\omega a/U_C) + iH_1^{(1)}(\omega a/U_C)\} , \quad (3.21)$$

$$x_1 \rightarrow a + 0, \quad x_2 = 0 ,$$

where $H_n^{(1)}$ are Hankel functions.

It follows from (3.15), (3.21) that at $K_3 = 0$ and fixed ω , the Kutta condition will be satisfied provided $\partial B'_s / \partial x_2 + \partial B'_\Omega / \partial x_2$ remains finite as $x_1 \rightarrow a + 0$, $x_2 = 0$. This will evidently be the case if

$$\gamma_o(\omega, 0) = \frac{-4\omega \{J_0(\omega a/U) + iJ_1(\omega a/U)\}}{\{H_0^{(1)}(\omega a/U_c) + iH_1^{(1)}(\omega a/U_c)\}} \int_{-\infty}^{\infty} \frac{\hat{\Omega}_3(\omega/U, K_2, 0) dK_2}{\omega^2 + U^2 K_2^2} . \quad (3.22)$$

The acoustic pressure fluctuations $p_s(\underline{x}, t)$ produced by the wake at large distances from the airfoil may be calculated from (3.3), (3.4) by replacing Ω_3 by Ω_{s3} and the convection velocity U (displayed explicitly on the right hand side of (3.3)) by U_c . The result can be expressed in terms of $\gamma_o(\omega, 0)$ by making use of (3.16), (3.17):

$$p_s(\underline{x}, t) = \frac{\pi \rho_o a U_c \cos \bar{\theta}}{4c|\underline{x}|} \frac{\partial}{\partial t} \int_{-\infty}^{\infty} \gamma_o(\omega, 0) H_1^{(1)}(\omega a/U_c) e^{-i\omega[t]} d\omega , \quad (3.23)$$

i.e., using (3.22),

$$p_s(\underline{x}, t) = \frac{-\pi \rho_o a U_c \cos \bar{\theta}}{c|\underline{x}|} \frac{\partial}{\partial t} \int_{-\infty}^{\infty} \frac{\omega \hat{\Omega}_3(\omega/U, K_2, 0) H_1^{(1)}(\omega a/U_c)}{(\omega^2 + U^2 K_2^2)} \times \frac{\{J_0(\omega a/U) + iJ_1(\omega a/U)\} e^{-i\omega[t]}}{\{H_0^{(1)}(\omega a/U_c) + iH_1^{(1)}(\omega a/U_c)\}} dK_2 d\omega . \quad (3.24)$$

This is a generalization of the formula that obtains on the basis of conventional thin airfoil theory, in which one takes $U_c = U$. Making the latter substitution in (3.24), combining the resulting expression with the direct radiation $p_\Omega(\underline{x}, t)$ given by

(3.8), and making use of a well known Wronskian identity for Bessel functions (Abramowitz and Stegun 1972, Section 9.1.17), we obtain

$$p(\underline{x}, t) = p_{\Omega}(\underline{x}, t) + p_s(\underline{x}, t)$$

$$= \frac{2i\rho_o U^2 \cos\bar{\theta}}{c|\underline{x}|} \frac{\partial}{\partial t} \int_{-\infty}^{\infty} \frac{\hat{\Omega}_3(\omega/U, K_2, 0) e^{-i\omega[t]} dK_2 d\omega}{(\omega^2 + U^2 K_2^2) \{H_0^{(1)}(\omega a/U) + iH_1^{(1)}(\omega a/U)\}} . \quad (3.25)$$

This expression for the net acoustic radiation is applicable when the wake vorticity is assumed to convect at the main stream velocity U , and involves the Sears function

$$S(x) = 2/\pi x \{H_0^{(1)}(x) + iH_1^{(1)}(x)\} ,$$

which arises in classical, incompressible thin airfoil theory (Sears 1940).

3.3 Summary of Results

For ease of reference we now collect together the formulae derived above for the two principal components of the vortex-airfoil interaction radiation:

The direct radiation $p_{\Omega}(\underline{x}, t)$:

$$p_{\Omega}(\underline{x}, t) = \frac{\pi \rho_0 a U \cos \bar{\theta}}{c |\underline{x}|} \frac{\partial}{\partial t} \int_{-\infty}^{\infty} \frac{\hat{\omega} \hat{\Omega}_3(\omega/U, K_2, 0) J_1(\omega a/U) e^{-i\omega[t]}}{(\omega^2 + U^2 K_2^2)} dK_2 d\omega . \quad (3.26)$$

The wake generated sound $p_S(\underline{x}, t)$:

$$p_S(\underline{x}, t) = \frac{-\pi \rho_0 a U_c \cos \bar{\theta}}{c |\underline{x}|} \frac{\partial}{\partial t} \int_{-\infty}^{\infty} \frac{\hat{\omega} \hat{\Omega}_3(\omega/U, K_2, 0) H_1^{(1)}(\omega a/U_c)}{(\omega^2 + U^2 K_2^2)} \times \frac{\{J_0(\omega a/U) + iJ_1(\omega a/U)\} e^{-i\omega[t]}}{\{H_0^{(1)}(\omega a/U_c) + iH_1^{(1)}(\omega a/U_c)\}} dK_2 d\omega . \quad (3.27)$$

4. ANALYTICAL SPECIFICATION OF A RECTILINEAR VORTEX

The above formulae will be applied to the case of a rectilinear vortex that is convected at the mean flow velocity U and "chopped" by a stationary airfoil. In the potential flow region the vortex has circulation Γ and there is a finite axial velocity (defect) within the core.

Let the axis of the vortex be in the direction of the unit vector \underline{n} whose orientation is specified by spherical polar angles (θ, ϕ) with respect to the uniformly translating coordinate system $\underline{x}' = \underline{x} - (Ut, 0, 0)$, introduced in Section 3. The angle θ is measured from the positive x'_3 -axis, and ϕ is the longitude measured from the x'_1 direction, as illustrated in Figure 3, such that

$$\underline{n} = (n_1, n_2, n_3) = (\sin\theta\cos\phi, \sin\theta\sin\phi, \cos\theta) . \quad (4.1)$$

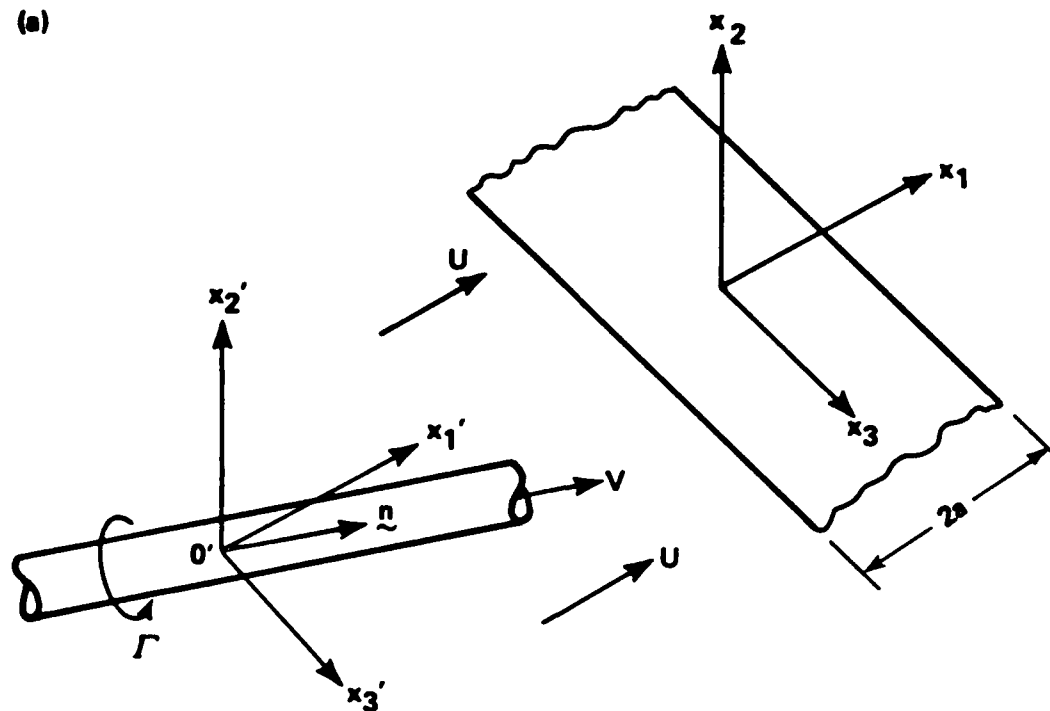
The origin O' of the moving coordinate system lies on the axis of symmetry of the vortex, translates at the convection speed U along the x_1 -axis and coincides with the fixed origin O at time $t = 0$.

There are two components of the vorticity distribution. The first is the axial vorticity $\underline{\Omega}_\Gamma$ which is parallel to \underline{n} and will be taken to be given by

$$\underline{\Omega}_\Gamma = \frac{\Gamma \underline{n} \exp\{-(r/R)^2\}}{\pi R^2} \quad (4.2)$$

where R is the nominal radius of the core of the vortex, and r denotes perpendicular distance from the uniformly translating axis of symmetry of the core. The Fourier transform $\hat{\underline{\Omega}}_\Gamma(K)$ of $\underline{\Omega}_\Gamma$ is defined as in (3.5), and is readily computed by transforming from the integration variables x'_1, x'_2, x'_3 to cylindrical polar

(b)



(b)

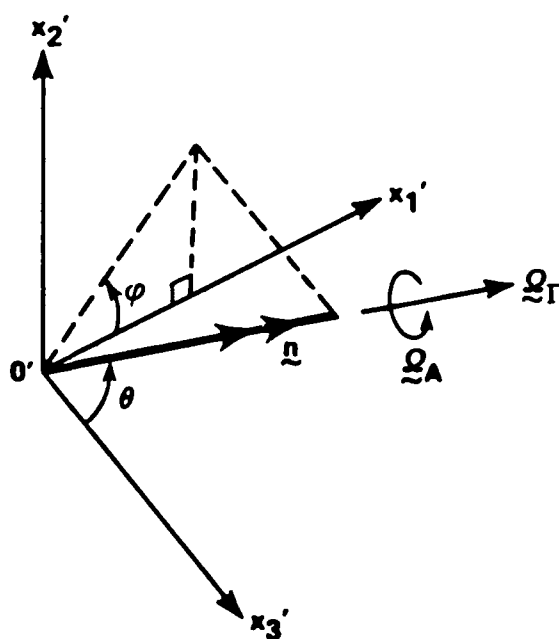


FIGURE 3. (a) COORDINATES DEFINING THE ORIENTATION OF THE IMPINGING VORTEX.
(b) COMPONENTS OF \underline{n} .

coordinates whose axis of symmetry coincides with that of the vortex. In this way one finds

$$\hat{\underline{\Omega}}_{\underline{r}}(\underline{K}) = \frac{\Gamma \underline{n}}{4\pi^2} \delta(\underline{n} \cdot \underline{K}) \exp\{-(KR/2)^2\}, \quad K = |\underline{K}|. \quad (4.3)$$

Second, in the presence of a mean axial flow within the core of the vortex (corresponding to an axial velocity defect), there will exist an azimuthal component of vorticity $\underline{\Omega}_A$. Let V denote the maximum axial velocity (defect), and assume that the local axial velocity \underline{v}_A may be taken in the form

$$\underline{v}_A = V \underline{n} \exp\{-(r/R)^2\}, \quad (4.4)$$

so that the axial volume flux is just equal to $\pi R^2 V$. In practice the axial flow core radius R in (4.4) will probably differ from the axial vorticity radius of (4.2), but such refinements will be ignored.

The Fourier transform of $\underline{v}_A(\underline{x}')$ is similar in form to (4.3), viz.,

$$\hat{\underline{v}}_{\underline{A}}(\underline{K}) = \frac{nVR^2}{4\pi} \delta(\underline{n} \cdot \underline{K}) \exp\{-(KR/2)^2\} \quad (4.5)$$

from which it is immediately deduced that,

$$\begin{aligned} \hat{\underline{\Omega}}_A(\underline{K}) &= i \underline{K} \wedge \hat{\underline{v}}_A(\underline{K}) \\ &= \frac{iVR^2}{4\pi} \underline{K} \wedge \underline{n} \delta(\underline{n} \cdot \underline{K}) \exp\{-(KR/2)^2\}. \end{aligned} \quad (4.6)$$

For future reference, we record the following particular components of (4.3), (4.6):

$$\hat{\Omega}_{\Gamma 3}(K_1, K_2, 0) = \frac{\Gamma n_3}{4\pi^2} \delta(n_1 K_1 + n_2 K_2) \exp\{-(K_1 R/2\sin\phi)^2\} ; \quad (4.7)$$

$$\hat{\Omega}_{A3}(K_1, K_2, 0) = \frac{iVR^2(n_1^2 + n_2^2)}{4\pi n_2} K_1 \delta(n_1 K_1 + n_2 K_2) \exp\{-(K_1 R/2\sin\phi)^2\} . \quad (4.8)$$

5. VORTEX CHOPPING NOISE

The results of Sections 3 and 4 will now be used to derive analytical representations of the acoustic pressure when the vortex core diameter $2R$ is small compared to the chord $2a$ of the airfoil. This condition is fulfilled by the experiments of Schlinker and Amiet (1983) and Ahmadi (1986).

5.1 Sound Generated by the Axial Component of Vorticity \underline{g}_T

Consider first the direct component of the radiation, defined by equation (3.26). Substituting for \hat{n}_3 from (4.7), performing the integration with respect to K_2 and the differentiation with respect to the time, we find

$$p_{T\Omega}(\underline{x}, t) = \frac{-i\rho_0 a U r \cos\theta |\sin\phi|}{4\pi c |\underline{x}| \tan\theta} \int_{-\infty}^{\infty} J_1(\omega a/U) \exp\{-(\omega R/2U \sin\phi)^2 - i\omega[t]\} d\omega. \quad (5.1)$$

In order to obtain the leading approximation to this integral when $R \ll a$, observe first that $2R/|\sin\phi|$ is precisely equal to the minimum interval in the x_1 -direction that contains the whole of the projected area of the vortex cross-section on the x_2 -plane of the airfoil. In the absence of contributions from the wake vorticity, the principal radiated pressure fluctuations are expected to be generated when the projected area is swept over the leading and trailing edges of the airfoil, and will be characterized by frequencies $\omega \sim U|\sin\phi|/R$. The waveform of the radiated sound should therefore be more sharply peaked when $|\phi| \sim \pi/2$. If it is assumed that $|\sin\phi| = O(1)$, which is typically the case when the core is "chopped," it follows that the dominant frequencies satisfy $\omega a/U \gg 1$. Introducing the change of variable

$$\lambda = \omega R/2U |\sin\phi|, \quad (5.2)$$

in (5.1) we conclude that the rapid variations and principal components of the acoustic signature are associated with contributions to the integral from the region $\lambda \approx 0(1)$. The argument of the Bessel function becomes $2\lambda a/R|\sin\phi| \gg 1$ for $\lambda \sim 0(1)$. The integrand may accordingly be simplified by use of the asymptotic approximation

$$J_1(x) \approx \text{sgn}(x) \{2/\pi|x|\}^{1/2} \sin\{|x| - \pi/4\}, \quad |x| \gg 1,$$

for real values of x , following which one finds

$$p_{r\Omega}(\underline{x}, t) \approx \frac{\rho_0 U^2 r \cos\theta |\sin\phi|^{3/2} (a/\pi R)^{1/2}}{8c|\underline{x}|\tan\theta} \{f(\alpha_+) - f(\alpha_-)\}, \quad (5.3)$$

where,

$$\alpha_{\pm} = (2a|\sin\phi|/R)\{1 \pm U[t]/a\}, \quad (5.4)$$

and,

$$f(\alpha) = \frac{8}{\pi} \int_0^{\infty} \cos\{\alpha u^2 - \pi/4\} \exp\{-u^4\} du. \quad (5.5)$$

The value of this integral can be expressed in terms of the modified Bessel functions $I_{\pm 1/4}$ (Gradshteyn and Ryzhik 1980, page 485):

$$f(\alpha) = |\alpha|^{1/2} \exp(-\alpha^2/8) \{I_{-1/4}(\alpha^2/8) + \text{sgn}(\alpha) I_{1/4}(\alpha^2/8)\}. \quad (5.6)$$

However, a more convenient formula, both for numerical and analytical purposes, is obtained by replacing the Bessel

functions by their representations in terms of the Kummer confluent hypergeometric function $M(a,b,z)$, defined by

$$M(a,b,z) = 1 + \frac{a}{b} \frac{z}{1!} + \frac{a(a+1)}{b(b+1)} \frac{z^2}{2!} + \dots, \quad (5.7)$$

namely (Abramowitz and Stegun 1972, Section 9.6.47):

$$I_\nu(z) = \frac{(z/2)^\nu e^{-z}}{\Gamma(1+\nu)} M(\nu+1/2, 2\nu+1, 2z), \quad (5.8)$$

where $\Gamma(x)$ denotes the Euler gamma function. This leads to

$$\begin{aligned} f(\alpha) &= \exp(-\alpha^2/4) \left\{ \frac{2}{\Gamma(3/4)} M(1/4, 1/2, \alpha^2/4) + \frac{\alpha}{2\Gamma(5/4)} M(3/4, 3/2, \alpha^2/4) \right\} \\ &= \frac{2}{\Gamma(3/4)} M(1/4, 1/2, -\alpha^2/4) + \frac{\alpha}{2\Gamma(5/4)} M(3/4, 3/2, -\alpha^2/4). \end{aligned} \quad (5.9a,b)$$

The first of these expressions is suitable for numerical work, and the second is obtained by use of the Kummer transformation $e^{-z}M(a,b,z) = M(b-a,b,z)$.

The function $f(\alpha) > 0$, and has a single maximum in the neighborhood of the origin. Thus, equation (5.3) indicates that the signature of the directly radiated sound $p_{r\Omega}(\underline{x},t)$ exhibits equal and opposite pulses respectively at $U[t]/a = \mp 1$, i.e., when the retarded position of the core of the vortex is in the immediate vicinities of the leading and trailing edges of the airfoil. It is also evident from (5.3) that the signs of these pressure peaks change as the polar angle θ made by the axial vorticity vector $\underline{\Omega}_r$ with the positive x_3 -direction increases through $\pi/2$ (and that the radiation is null when $\theta = \pi/2$), although the shape of the pulses depends on the value of ϕ but not

0. The double pulse profile is illustrated by the dashed curve in Figure 4, which depicts the variation of

$$c|\underline{x}|p_{r\Omega}(\underline{x},t)/\rho_0 U^2 r \cos \bar{\theta} ,$$

as determined by (5.3) for $\theta = 85^\circ$, $\phi = 90^\circ$, and $R/a = 0.1$, as a function of the retarded position $U[t]/a$ of the center of the vortex in the plane of the airfoil scaled on the semi-chord a .

These detailed predictions are, however, unrealistic inasmuch as they take no account of the influence of induced vortex shedding from the trailing edge. The radiation from the latter is determined by equation (3.27), in which $\hat{\Omega}_3$ is given by (4.7), and an explicit representation of its contribution when $R \ll a$ can be derived in the manner described above, leading to

$$p_{rs}(\underline{x},t) \approx \frac{\rho_0 U U_c r \cos \bar{\theta} |\sin \phi|^{3/2} (a/\pi R)^{1/2} f(\alpha_-)}{8c|\underline{x}| \tan \theta} . \quad (5.10)$$

Evidently, this is significantly different from zero only when the retarded position of the vortex is close to the trailing edge (i.e., when $\alpha_- \approx 0$).

The net acoustic pressure is obtained by combining this result with the representation (5.3) of the direct radiation, which yields:

$$p_r(\underline{x},t) \approx \frac{\rho_0 U^2 r \cos \bar{\theta} |\sin \phi|^{3/2} (a/\pi R)^{1/2}}{8c|\underline{x}| \tan \theta} \{f(\alpha_+) - (1-U_c/U)f(\alpha_-)\} . \quad (5.11)$$

This formula reveals that, when the wake convection velocity U_c is equal to the main stream velocity U , the radiation produced by the

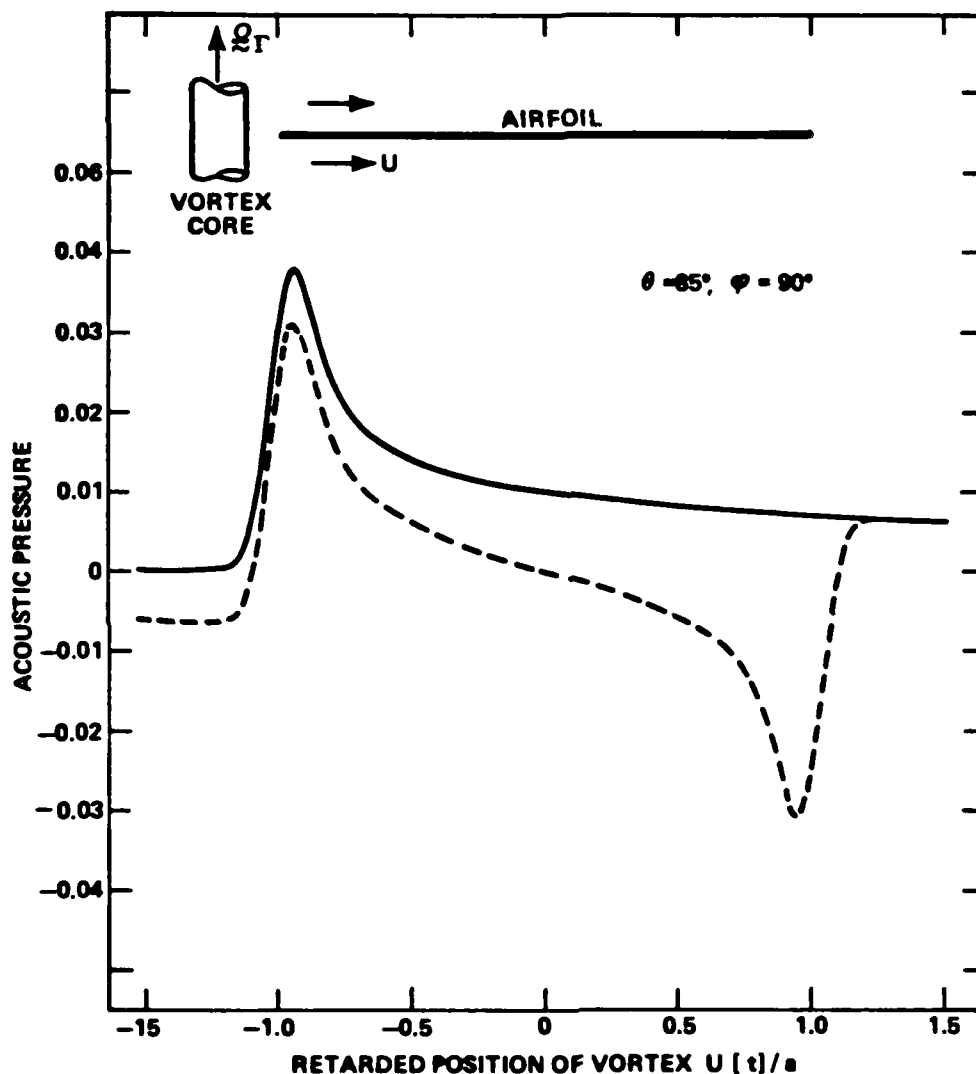


FIGURE 4. FAR FIELD ACOUSTIC PRESSURE PROFILES GENERATED BY THE AXIAL COMPONENT OF VORTICITY $\underline{\omega}_r$ FOR $R/a = 0.1$, $\theta = 85^\circ$, AND $\phi = 90^\circ$. — — —, THE DIRECT RADIATED SOUND: $c|\underline{x}|p_{r\Omega}(\underline{x}, t)/\rho_0 U^2 r \cos \bar{\theta}$; ——— THE NET RADIATION: $c|\underline{x}|p_r(\underline{x}, t)/\rho_0 U^2 r \cos \bar{\theta}$ WHEN THE WAKE CONVECTION VELOCITY $U_c = U$.

wake exactly cancels the directly generated acoustic pulse from the trailing edge. In that case, the pressure signature has a single peak which is generated as the vortex core sweeps across the leading edge of the airfoil, as illustrated by the solid curve in Figure 4. The shape of this curve is similar to the pressure profiles computed numerically (by Fast Fourier transform) by Amiet (1986). In practice it is likely that $U_c < U$; typically in the near wake $U_c \approx 0.8U$. The directly generated trailing edge pulse is then only partially destroyed by the shed vorticity. This will be discussed further in Section 6. When $U_c \rightarrow 0$, the hydrodynamic wavelength of the wake vorticity ultimately vanishes, and the prediction (5.11) reduces to that applicable when the Kutta condition is not imposed. These conclusions are analogous to results previously given by Howe (1976) for two-dimensional edge noise problems.

The widths of the acoustic pulses increase both as R/a increases and also when $|\sin\phi|$ decreases from unity. The effect of this latter variation is demonstrated in Figure 5, which depicts profiles of $p_r(\underline{x}, t)$ for $R/a = 0.1$, $U_c = U$, $\theta = 85^\circ$, and $\phi = 30^\circ, 60^\circ, 90^\circ$.

5.2 Sound Generated by the Axial Velocity Defect in the Core ($\underline{\Omega}_A$)

The substitution of the component (4.8) of the azimuthal vorticity into equations (3.26), (3.27) enables integral representations to be derived for the directly generated and wake generated acoustic pressures produced by the axial velocity \underline{v}_A in the core of the vortex. When $R/a \ll 1$ the values of these integrals can be estimated by means of the procedure described above. It is then found that the net acoustic pressure $p_A(\underline{x}, t)$ can be expressed in the form

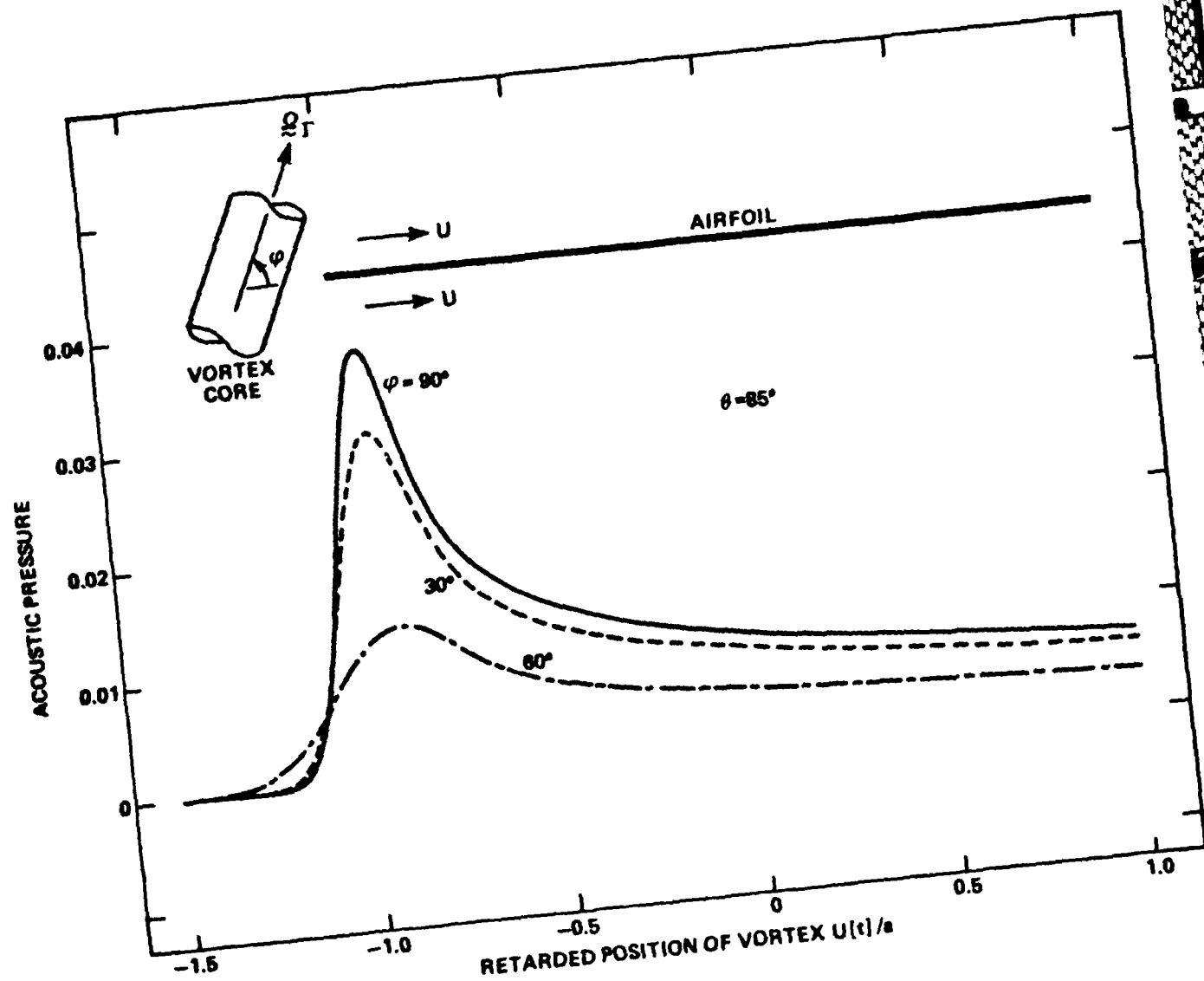


FIGURE 5. PROFILES OF THE ACOUSTIC PRESSURE $c|\underline{x}|p_\Gamma(\underline{x},t)/\rho_0 U^2 r \cos \bar{\theta}$ FOR $R/a = 0.1$, $U_C = U$, $\theta = 85^\circ$, AND DIFFERENT VALUES OF ϕ .

$$p_A(\underline{x}, t) = \frac{-\rho_0 U^2 V \cos \bar{\theta} \sin \phi |\sin \phi|^{1/2} (\pi a R)^{1/2}}{4c |\underline{x}|} \times \{f'(\alpha_+) + (1 - U_c/U) f'(\alpha_-)\} , \quad (5.12)$$

where α_{\pm} , $f(\alpha)$ are defined as in (5.4), (5.5), and $f'(\alpha) = \partial f(\alpha)/\partial \alpha$. This derivative is readily evaluated from the representation (5.9b) by making use of the relation

$$\frac{\partial M}{\partial z}(a, b, z) = \frac{a}{b} M(1+a, 1+b, z)$$

(Abramowitz and Stegun 1972, Section 13.4.8), yielding

$$f'(\alpha) = \frac{\exp(-\alpha^2/4)}{2} \{M(3/4, 3/2, \alpha^2/4)/\Gamma(5/4) - \alpha M(1/4, 3/2, \alpha^2/4)/\Gamma(3/4) - \alpha^2 M(3/4, 5/2, \alpha^2/4)/4\Gamma(5/4)\} . \quad (5.12)$$

It is clear from (5.12) that the pressure profile is independent of the angle θ between the velocity defect \underline{v}_A and the x_3 -axis (in the spanwise direction). This is because the acoustic dipole source is equivalent to two equal and opposite monopole sources on the upper and lower surfaces of the airfoil whose strengths are proportional to the volume flux in the x_2 -direction in the core of the vortex, and (except in the singular cases $\theta = 0, \pi$) this does not depend on the orientation of the vortex. The formula for the directly generated sound $p_{A\Omega}(\underline{x}, t)$, which is applicable when vortex shedding from the trailing edge is ignored, is obtained by setting $U_c = 0$ in (5.12). The corresponding profile of the pressure field has the symmetric form illustrated by the dashed curve in Figure 6 for $R/a = 0.1$ and $\phi = 90^\circ$. The identical, but time-reversed double pulses are generated during the passage of the vortex over the leading and trailing edges of the airfoil. When the Kutta condition is imposed with $U_c = U$, the trailing edge pulse is

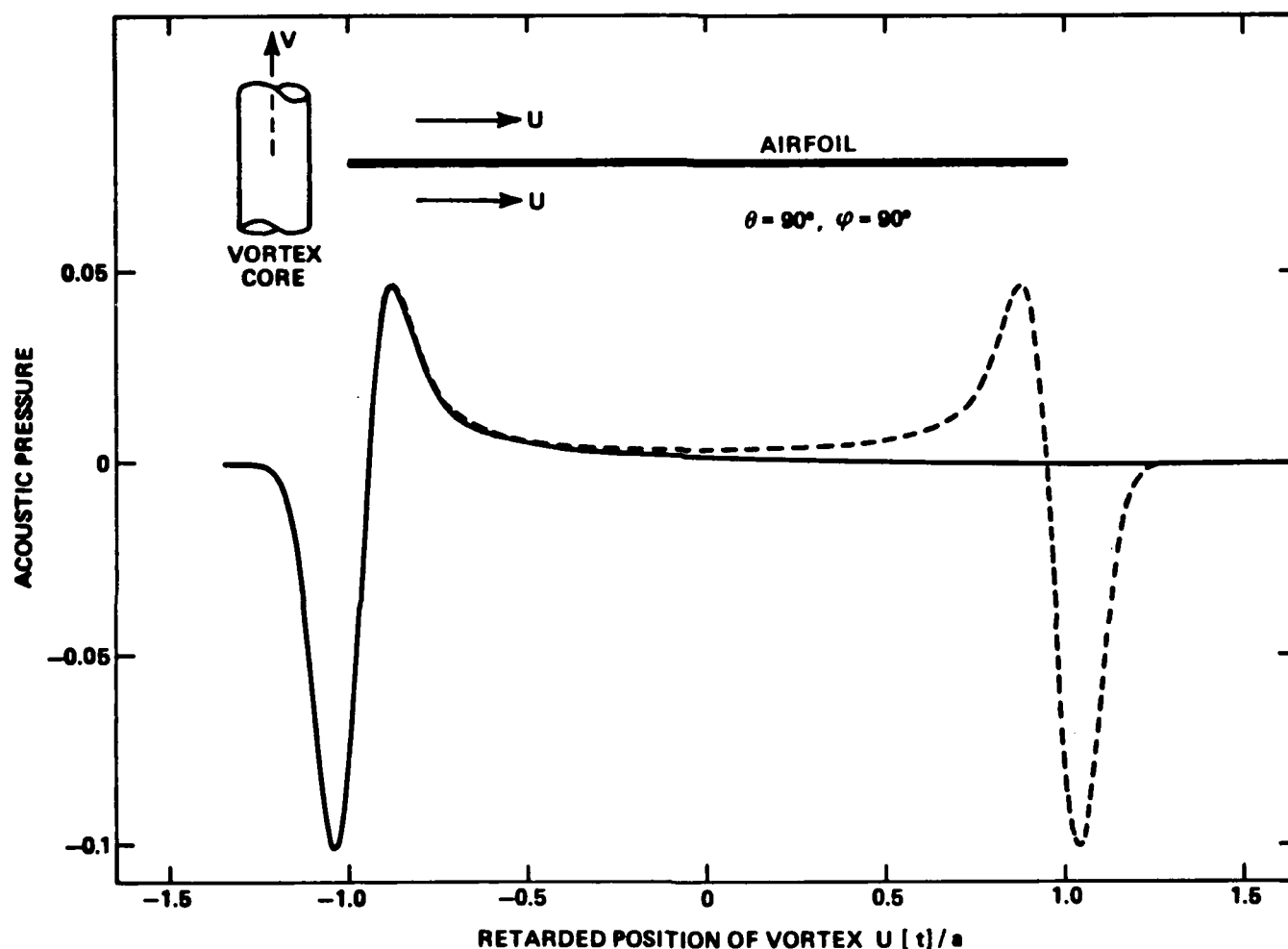


FIGURE 6. FAR FIELD ACOUSTIC PRESSURE PROFILES GENERATED BY THE AXIAL VELOCITY DEFECT \underline{v}_A FOR $R/a = 0.1$, $\phi = 90^\circ$.
 — — —, THE DIRECT RADIATED SOUND:
 $cp_{A\Omega}(\underline{x}, t)/\rho_o U^2 V(a/|\underline{x}|) \cos \bar{\theta}$; ———, THE NET RADIATION:
 $cp_A(\underline{x}, t)/\rho_o U^2 V(a/|\underline{x}|) \cos \bar{\theta}$ WHEN THE WAKE CONVECTION VELOCITY $U_c = U$.

annihilated by destructive interference with the wake generated sound, and the acoustic signature has the form shown by the solid curve in the Figure. When $0 < U_c < U$, the trailing edge pulse is only partially destroyed.

As in the case of the radiation produced by the axial component $\underline{\Omega}_r$ of vorticity, the width of the acoustic pressure pulses is governed by the magnitude of $R|\sin\phi|/a$. This is illustrated in Figure 7 when $R/a = 0.1$, $U_c = U$, and for different values of ϕ .

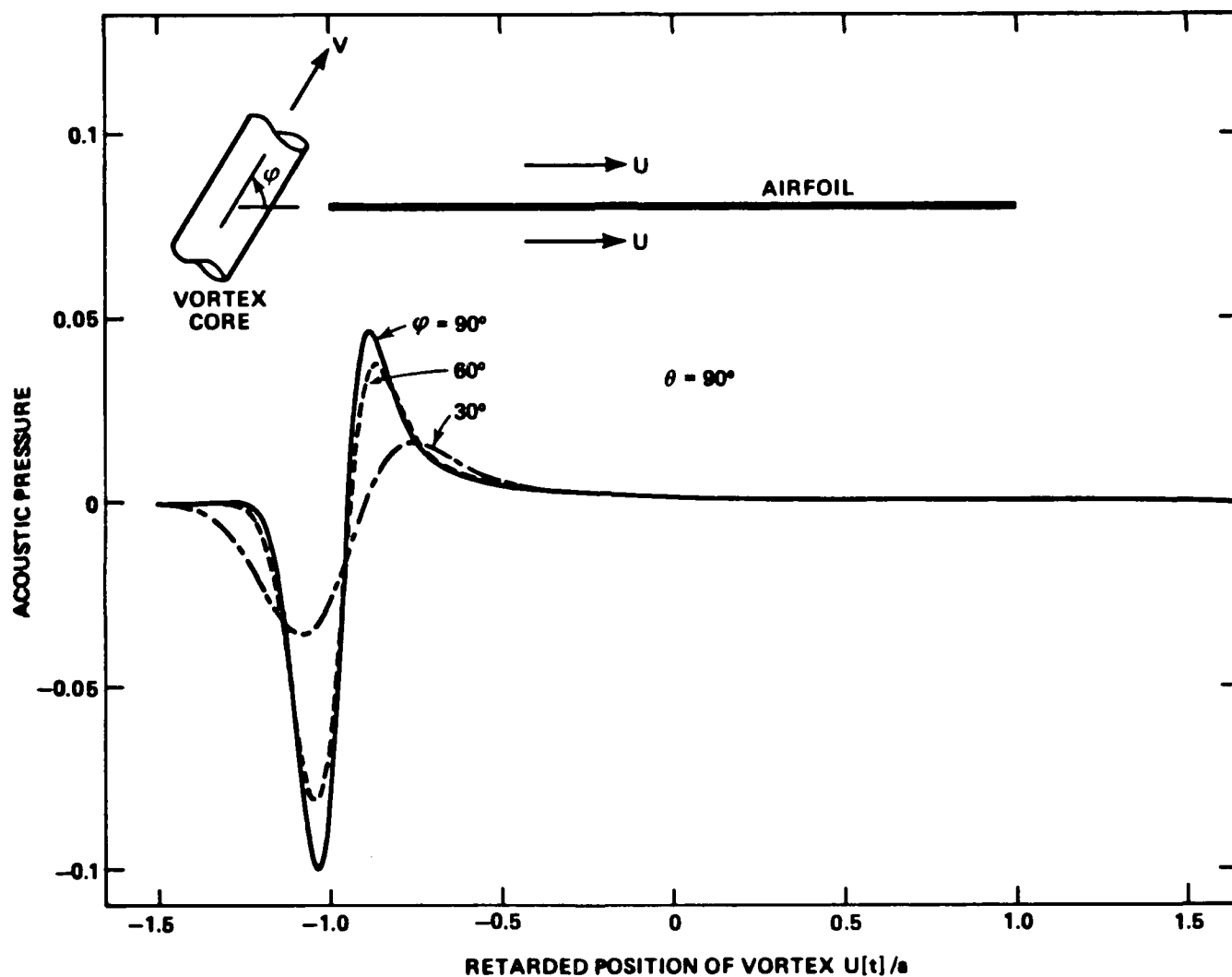


FIGURE 7. PROFILES OF THE ACOUSTIC PRESSURE $cp_A(\underline{x}, t)/\rho_0 U^2 V(a/|x|)\cos\theta$ FOR $R/a = 0.1$, $U_c = U$, AND DIFFERENT VALUES OF ϕ .

6. APPLICATION TO ROTOR-VORTEX INTERACTION NOISE

The sound produced when the tip vortex from an airfoil is periodically "chopped" by a rotor has been examined experimentally by Schlinker and Amiet (1983) and by Ahmadi (1986). The experimental configurations of both investigations are depicted schematically in Figure 8. A trailing vortex is produced in low Mach number air flow in an open-jet wind tunnel by an airfoil A set at a finite angle of attack. The vortex encounters a rotor at the downstream station B, whose plane of rotation is perpendicular to the mean flow. Observations are made of the vortex-rotor interaction noise by filtering from the received signal the (typically much stronger) dipole radiation that is generated by the accelerating mean pressure loading forces on the rotor blades.

In order to apply the theory of Section 2 to this experiment it is strictly necessary to take account of the finite span of the rotor blades, and of the influence on the higher frequency components of the radiated sound of their non-compact chords. The present discussion will, however, be based on the detailed predictions made in Section 5 for a flat strip airfoil of infinite span. Finite span effects are probably unimportant provided that, in the region where the vortex is cut by the airfoil, the length scale of variation of the chord in the spanwise direction is large relative to the diameter of the core.

Let U_0 denote the mean velocity in the wind tunnel, and introduce parameters β , γ such that the vortex strength Γ (defined as in equation (4.2)), and the axial flow velocity defect reference speed V (of equation (4.4)) are given by

$$\Gamma = 4\pi a U_0 \beta, \quad V = -\gamma U_0, \quad (6.1)$$

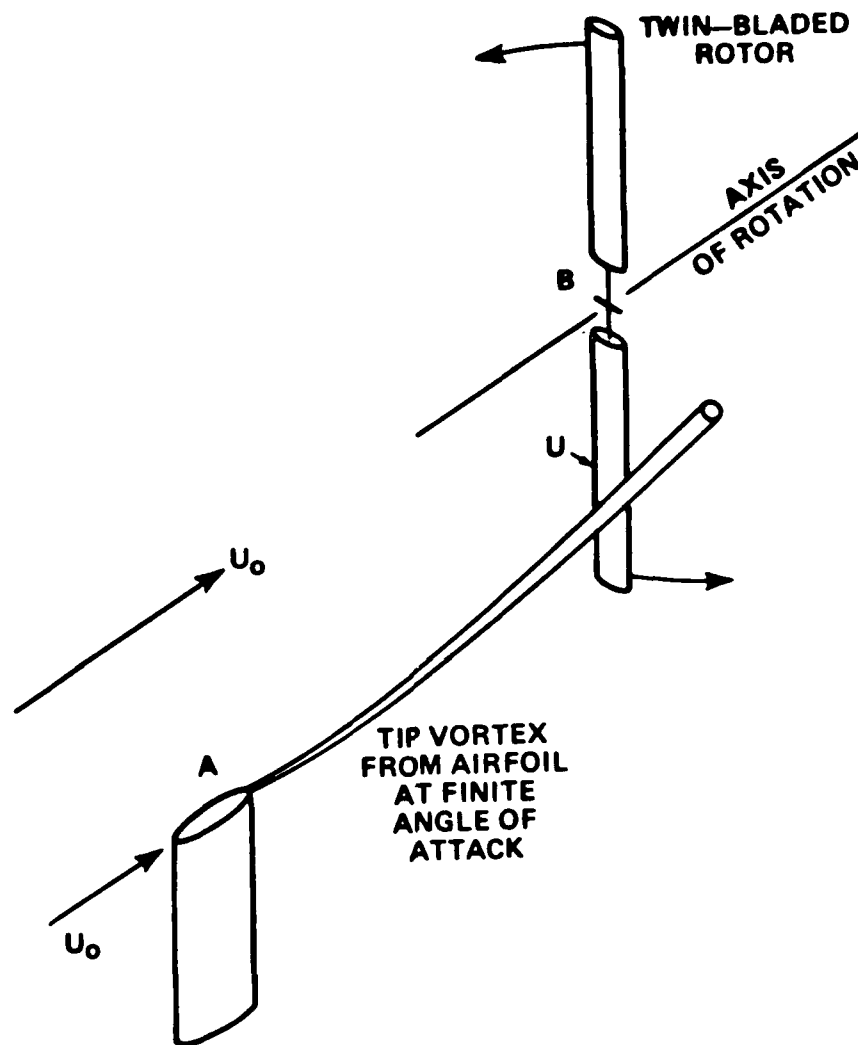


FIGURE 8. SCHEMATIC EXPERIMENTAL ARRANGEMENT FOR STUDYING VORTEX-ROTOR INTERACTION NOISE.

where $2a$ is the chord of a rotor blade. For the experimental arrangement of Figure 8, β and γ are both positive. Thus, the maximum axial velocity defect within the core (which, of course, refers to the maximum core velocity relative to the ambient flow velocity U_0) is negative. According to Schlinker and Amiet (1983), γ is typically of order 0.1.

The formulae derived in Section 5 for the vortex-chopping noise should be applicable provided that $M = U/c \ll 1$, where U is now the chordwise component of the velocity of the airfoil (i.e., of the rotor blade) relative to the vortex at the spanwise location at which the vortex is cut by a rotor. Thus, using the definitions (6.1) in equations (5.11), (5.12), the acoustic pressure in the far field may be cast in the form

$$p(\underline{x}, t) = p_r(\underline{x}, t) + p_A(\underline{x}, t) \quad (6.2)$$

where,

$$\begin{aligned} & \frac{p_r(\underline{x}, t)}{\rho_0 U^2 M_0 \cos \bar{\theta} (a/|\underline{x}|)} \\ &= \frac{\beta |\sin \phi|^{3/2} (\pi a/R)^{1/2}}{2 \tan \theta} \{f(\alpha_+) - (1 - U_c/U) f(\alpha_-)\} , \end{aligned} \quad (6.3)$$

$$\begin{aligned} & \frac{p_A(\underline{x}, t)}{\rho_0 U^2 M_0 \cos \bar{\theta} (a/|\underline{x}|)} \\ &= \frac{\gamma}{4} \sin \phi |\sin \phi|^{1/2} (\pi R/a)^{1/2} \{f'(\alpha_+) + (1 - U_c/U) f'(\alpha_-)\} . \end{aligned} \quad (6.4)$$

In these expressions α_{\pm} , $f(\alpha)$, $f'(\alpha)$ are respectively defined by equations (5.4), (5.9), (5.13), and $M_0 = U_0/c$.

The contribution $p_r(x,t)$ of the radiation produced by the axial component of vorticity vanishes identically when $\theta = 90^\circ$ (when the axis of the vortex is normal to the plane of the rotor disc), and varies rapidly with θ in the neighborhood of this angle. In the experiments θ is typically close to 90° , so that reliable predictions can be made only when the orientation of the vortex with respect to a rotor blade is known precisely. This is illustrated in Figure 9, which depicts the individual waveforms p_A , p_r , $p_A + p_r$, for

$$\beta = 0.02, \gamma = 0.1, U_c/U = 1, \phi = 90^\circ,$$

and for $\theta = 85^\circ, 90^\circ, 95^\circ$. The profile of p_A is independent of θ , but that of p_r is inverted when θ changes from 85° to 95° . Accordingly, the net acoustic signature exhibits markedly different characteristics for relatively small variations in vortex orientation.

A tentative comparison of theory and experiment is made in Figure 10. Figure 10(a) shows detail of the vortex-airfoil interaction radiated pressure signature measured at a downstream station ($0 < \bar{\theta} < 90^\circ$) by Schlinker and Amiet (1983) at their Test Condition B. This corresponds approximately to

$$\beta = 0.3R/a, \gamma = 0.1, U = 155 \text{ msec}^{-1}. \quad (6.5)$$

The rotor blade chord $2a = 5.7$ cms, so that the duration of the interaction between the vortex and the airfoil is approximately equal to $2a/U \approx 0.3$ msec.

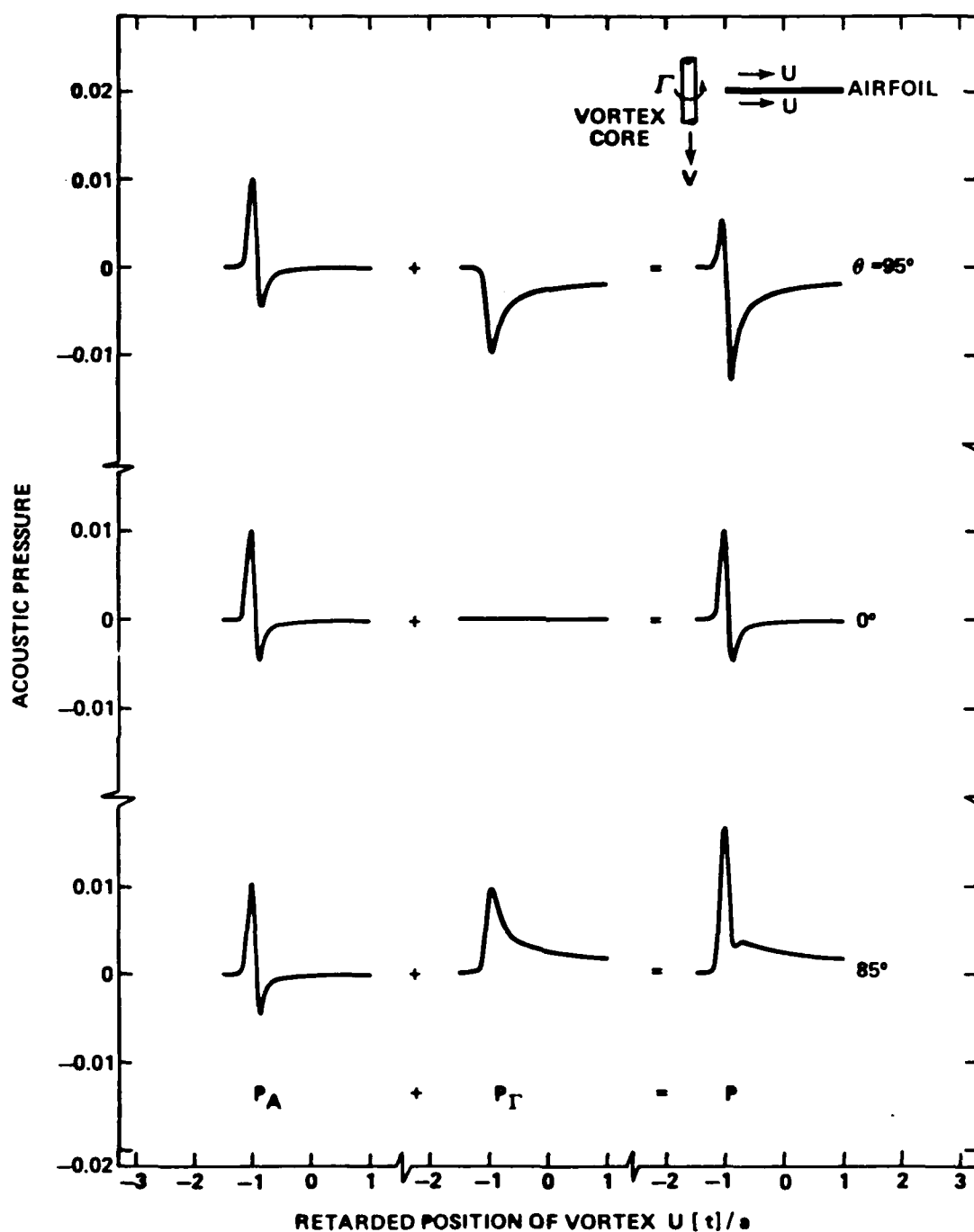


FIGURE 9. ILLUSTRATING THE CRITICAL DEPENDENCE OF THE NET ACOUSTIC PRESSURE SIGNATURE $p(\underline{x}, t)$ ON THE ORIENTATION OF THE VORTEX WHEN θ IS CLOSE TO 90° .

Corresponding pressure signatures predicted by (6.2) - (6.4) are illustrated in Figures 10(b), (c), respectively for $U_c/U = 1.0, 0.8$. We have taken $R/a = 0.15$, which is similar in magnitude to the value observed experimentally, and $\phi = 90^\circ$, $\theta = 95^\circ$. The physical scale of the axis defining the retarded position $U[t]/a$ of the vortex axis in the plane of the airfoil has been adjusted to be in approximate correspondence with the abscissa in Figure 10(a). In the experiment the values of the angles ϕ and θ which specify the orientation of the vortex were obtained from photographic records of smoke streaks in the core of the vortex. The degree of uncertainty in this procedure was not quantified, however, and the value of θ estimated by this means by Schlinker and Amiet (1983) was actually 104.5° . If that value had been used in plotting Figures 10(b), (c), the contribution $p_A(\underline{x}, t)$ from the axial velocity defect would have been small relative to $p_T(\underline{x}, t)$, and the positive peak at $U[t]/a \approx -1$ would have been very much smaller. In Figure 10(c) the secondary peak generated at the trailing edge of the airfoil ($U[t]/a \approx 1$) arises from the incomplete cancellation of the directly radiated sound by that produced by the wake. Its approximate correspondence with the trailing edge peak of Figure 10(a) suggests that the hypothesis that $U_c < U$ may be valid. The widths of the theoretically predicted pressure peaks are narrower than in the experiment. This is probably because of the assumption that the airfoil chord is acoustically compact, which is not strictly appropriate when, as in the experiment, the Mach number $M = U/c$ is as large as 0.45. According to the numerical results of Amiet (1986) non-compactness would be expected to broaden the pressure signature.

The positive pressure peaks generated at the leading and trailing edges of the airfoil are absent in the initial theoretical predictions of Schlinker and Amiet (1983) and Amiet (1986). These authors took no account of the axial velocity

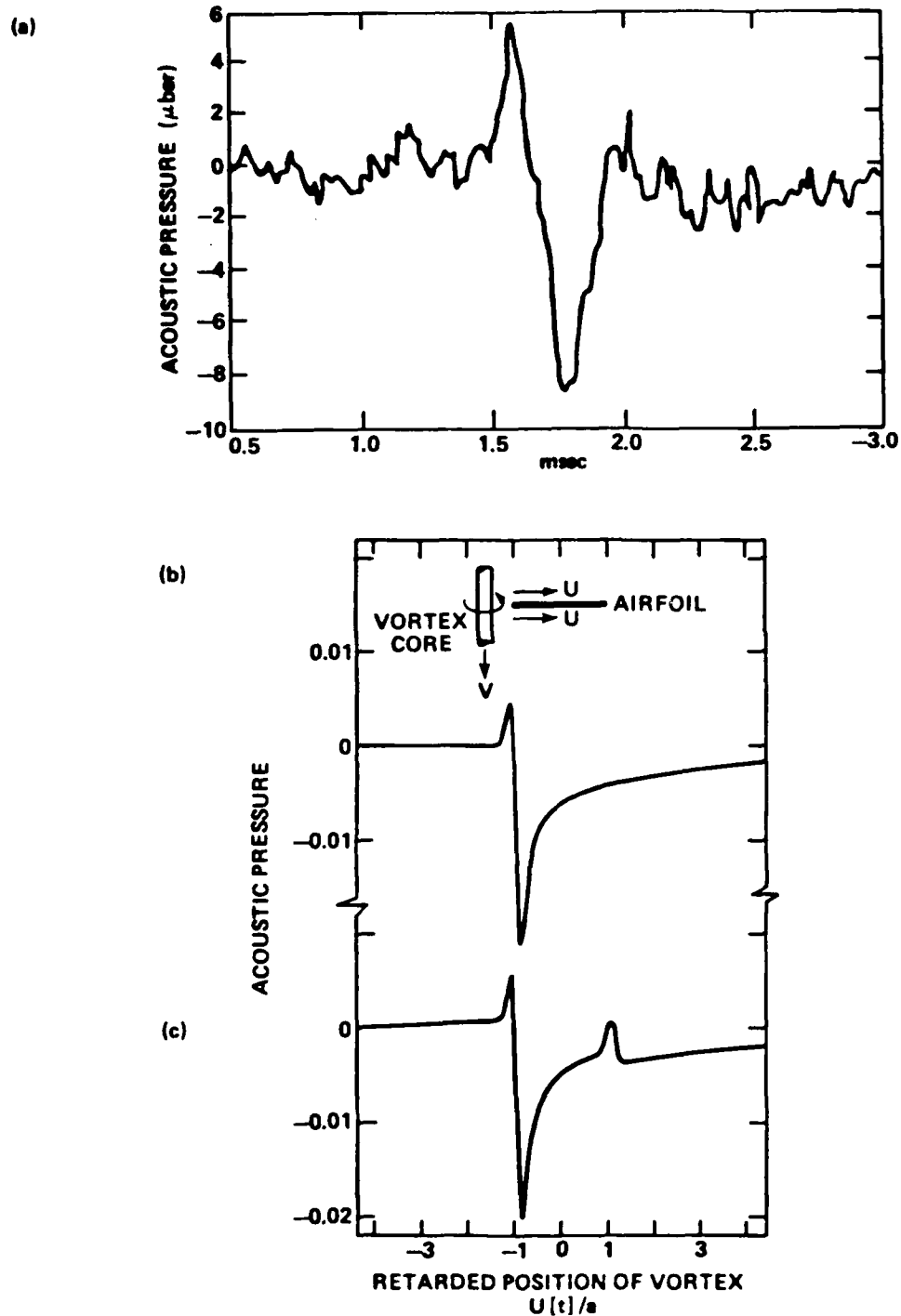


FIGURE 10. (a) TYPICAL ACOUSTIC PRESSURE SIGNATURE PRODUCED BY VORTEX-AIRFOIL INTERACTION IN TEST CONDITION B OF SHLINKER AND AMIET (1983). (b) THEORETICAL PREDICTION $p(\underline{x}, t)/\rho_0 U^2 M_0 \cos \theta (a/|\underline{x}|)$ FOR $U_c/U = 1$; (c) PREDICTION FOR $U_c/U = 0.8$.

defect in the vortex core, nor of the possibility that $U_c < U$. In order to obtain predictions that exhibit such peaks, they postulated that the azimuthal velocity v_r , say, induced by the axial component of vorticity $\underline{\Omega}_r$, will in practice decay more rapidly at large distance r from the axis than is implied by the potential flow formula $v_r = \Gamma/2\pi r$. Their hypothesis involved the assumption that the distribution of axial vorticity could be modelled by the formula

$$\underline{\Omega}_r = \frac{\Gamma}{\pi R^2} \left\{ [1 + (R/R_1)^2] \exp\{-(r/R)^2\} - (R/R_1)^2 \exp\{-(r/R_1)^2\} \right\} ,$$

(6.6)

instead of (4.2), where R_1 is an adjustable length scale which is taken to be equal to the chord $2a$ of the airfoil. A consequence of this modification of $\underline{\Omega}_r$ is that the net flux of vorticity through a plane at right angles to the axis of the vortex is identically zero, the direction of the vorticity vector changing sign at $r/R \approx 2.6$ when $R/a = 0.15$. This is unlikely to occur in practice, however, and must cast serious doubt on the validity of predictions based on (6.6).

7. CONCLUSION

There are two principal components of the sound produced when the core of a rectilinear vortex is "chopped" by an airfoil of large aspect ratio. These may be attributed to the axial and azimuthal distributions of vorticity, the latter being non-zero when there exists a finite axial velocity defect within the core. In practice the sound generated by the axial vorticity is usually dominant, except when the vortex is cut by an airfoil moving in a plane perpendicular to the vortex axis. In that case, the sound produced by the axial vorticity is effectively null.

The predicted profile of the acoustic pressure is dependent on the flow conditions assumed to obtain at the trailing edge of the airfoil. The impinging vortex induces vortex shedding from the edge into the wake, the strength of which is determined by application of the unsteady Kutta condition. Sound generated by the wake interferes destructively with that produced by the vortex sweeping past the trailing edge. If it is assumed that wake vorticity convects downstream at precisely the mean velocity of translation of the impinging vortex, the interference is complete, and for all practical purposes no sound emanates from the trailing edge. Most of the radiation is then associated with the vortex-airfoil interaction at the nose of the airfoil. The axial component of vorticity generates a single (compressive or rarefaction) pulse during this interaction, whereas the pressure signature produced by the azimuthal vorticity consists of a pulse followed by a larger pulse of opposite sign.

When the characteristic hydrodynamic length scales of fluid motion in the trailing edge region are small relative to the chord of the airfoil, and this is the case when the diameter of the vortex core is small, it is likely that vorticity in the wake

will convect at speeds that are less than in the free stream, at least in the near wake, where the most important interactions with the airfoil occur. In that case, complete cancellation of the vortex-generated sound at the trailing edge does not occur, and secondary acoustic pulses, of smaller amplitude than those from the leading edge, are produced. This hypothesis finds tentative support in the comparison in Section 6 of theoretical predictions with measurements of Schlinker and Amiet (1983).

Further developments of the theory are required to include the influences of:

1. Finite span of the airfoil. This is a straightforward extension of the work of Sections 2 and 3, whose principal difficulty will be the determination of appropriate potential functions γ_i of the low frequency Green's function.
2. Finite camber, twist and thickness of the airfoil. Differences in the mean flow velocities on the upper and lower surfaces of the airfoil will introduce a finite difference in the arrival times at the trailing edge of the upper and lower portions of the chopped vortex. This could produce interesting and perhaps noisy dynamical events in the wake, some of which have been revealed in the recent flow visualization studies of Cary (1987).
3. Finite distortion of the vortex on encountering the airfoil. This is important when the diameter of the core is comparable to the length scales of geometric features of the airfoil and of the mean flow over the airfoil (Goldstein and Atassi 1976). In addition, vortex distortion can generate bending waves and other hydrodynamic disturbances which propagate along the axis

of the vortex. "Vortex breakdown" may also occur if the duration of the vortex-airfoil interaction is sufficiently long.

4. Non-compact airfoil chord. This is unlikely to be important in underwater applications. Amiet (1986) has analyzed such effects for a flat plate airfoil of large aspect ratio when the wake vorticity convects at the velocity of the mean flow.

REFERENCES

- Abramowitz, M., and Stegun, I.A. 1972 Handbook of Mathematical Functions (10th corrected edition). Washington DC: U.S. Department of Commerce, National Bureau of Standards, Applied Math Series No. 55.
- Ahmadi, A.R. 1986 AIAA J. Aircraft 23, 47-55. An experimental investigation of blade-vortex interaction at normal incidence.
- Amiet, R.K. 1974 AIAA J. 12, 253-255. Compressibility effects in unsteady thin-airfoil theory.
- Amiet, R.K. 1976 AIAA J. 14, 541-542. Airfoil response to an incompressible skewed gust of small spanwise wavenumber.
- Amiet, R.K. 1986 J. Sound Vib. 107, 487-506. Airfoil gust response and the sound produced by airfoil-vortex interaction.
- Ashley, H., and Landahl, M. 1985 Aerodynamics of Winds and Bodies. New York: Dover Publications.
- Cary, C.M. 1987 NASA Contractor Report No. CR-177457. An experimental investigation of the chopping of helicopter main rotor tip vortices by the tail rotor,. Part II: High speed photographic study.
- Goldstein, M.E., and Atassi, H. 1976 J. Fluid Mech. 74, 741-765. A complete second order theory for the unsteady flow about an airfoil due to a periodic gust.
- Gradshteyn, I.S., and Ryzhik, I.M. 1980 Table of Integrals, Series, and Products, (corrected edition). New York: Academic Press.
- Gutin, L. 1948 NACA TN 1195. On the sound field of a rotating propeller.
- Hardin, J.C., and Lamkin, S.L. 1987 Trans. ASME, J. Vib., Acoust., Stress and Rel. Design, 109, 29-36. An Euler calculation of blade-vortex interaction noise.
- Howe, M.S. 1975 J. Fluid Mech. 71, 625-673. Contributions to the theory of aerodynamic sound, with application to excess jet noise and the theory of the flute.

- Howe, M.S. 1976 J. Fluid Mech. 76, 711-740. The influence of vortex shedding on the generation of sound by convected turbulence.
- Karman, Th. von, and Sears, W.R. 1938 J. Aero Sci. 5, 379-390. Airfoil theory for non-uniform motion.
- Lee, D.J., and Roberts, L. 1985 AIAA Paper 85-0004. Interaction of a turbulent vortex with a lifting surface.
- Leibovish, S., Brown, S.N., and Patel, Y. 1986 J. Fluid Mech. 173, 595-624. Bending waves on inviscid columnar vortices.
- Leverton, J.W., Pollard, J.S., and Wills, C.R. 1977 Vertica 1, 213-221. Main rotor/tail rotor interactions.
- Lighthill, M.J. 1958 An Introduction to Fourier Analysis and Generalized Functions. Cambridge University Press.
- Martinez, R., and Widnell, S.E. 1983 AIAA J. 21, 808-815. Aerodynamic theory for wing with side edge passing subsonically through a gust.
- Milne-Thomson, L.M. 1968 Theoretical Hydrodynamics, (5th edition). London: Macmillan.
- Schlinker, R.H., and Amiet, R.K. 1983 AIAA Paper 83 - 0720. Rotor-vortex interaction noise.
- Schmitz, F.H., and Yu, Y.H. 1986 Helicopter impulsive noise: theoretical and experimental status. In Recent Advances in Aeroacoustics (edited by Krothapally, A. and Smith, C.A.). New York: Springer-Verlag.
- Sears, W.P. 1940 J. Franklin Inst. 230, 95-111. Operational methods in the theory of airfoils in nonuniform motion.
- Stratton, J.A. 1941 Electromagnetic Theory. New York: McGraw-Hill.

END

DATE

FILMED

6-1988

DTic